HIGH-CURRENT ION INDUCTION LINAC FOR HEAVY ION FUSION: 2D3V NUMERICAL SIMULATION

O.V. Bogdan, V.I. Karas', E.A. Kornilov, O.V. Manuilenko*

National Science Center "Kharkov Institute of Physics and Technology", Kharkov, Ukraine,
****E-mail:ovm@kipt.kharkov.ua***

The 2d3v particle-in-cell simulations of the transport and acceleration of a high-current tubular ion beam through six magnetoinsulated accelerating gaps are presented. The ion beam is neutralized by an accompanying electron beam. The accelerating electric fields in the first, third, and fifth cusps are chosen so that electron beam kinetic energy is slightly higher than the potential barrier of the accelerating field in each cusp. The second, fourth, and sixth cusps are used for injection of additional high current electron beams. The accelerating fields in the second, fourth, and sixth cusps are zero. The simulations involve solving a complete set of Maxwell's equations with charge-conserving schemes for calculating the current density on a mesh, and relativistic motion equations for charged particles. It is shown, that at chosen acceleration rates the quality of ion distribution function on the accelerator exit is not worsened drastically in comparison with the transportation mode. It is shown, that the optimized in space and time injection of additional high current electron beams in cusps results in increase of accelerated ion beam monochromaticity and to reduction it divergency on an accelerator exit.

PACS: 41.75.-i, 52.40.Mj, 52.58.Hm, 52.59.-f, 52.65.Rr

1. INTRODUCTION

Two methods for producing high-current ion beams (HCIBs) by linacs are now being considered for applications in inertial confinement fusion (ICF) [1,2]. The first one is based on linear resonance accelerators with storage rings, and the second, on induction linacs. The disadvantage of the first approach is that beam pulse should be compressed in time by a factor of 10^5 in compression rings.

The method based on a vacuum induction linac (LIA) [1,2] implies the simultaneous acceleration of 16 to 120 ion beams in quadrupole lenses, where they are focused in the transverse direction. During the acceleration, the number of ion beams becomes smaller because some of them are merged into one. The final ion energy should be on the order of 10 GeV with an energy content on the order of 10 MJ, the pulse duration being several tens of nanoseconds. Another approach to using an LIA to generate HCIBs is to utilize not vacuum systems for transporting beams - quadrupoles and solenoids - but collective focusing techniques in which the space-charge forces of an ion beam are neutralized by electrons [2] and the electron current is suppressed by the magnetic insulation of the accelerating gaps. In such an LIA with charge- and current-neutralized HCIBs in magnetically insulated accelerating gap, the ion current during acceleration can be as high as tens of kA. For ICF purposes, this means that the final ion energy can be lowered to several hundreds of MeV, while keeping the required energy content of the beams on the target unchanged [2]. In addition, there is no need in storage complexes.

The mechanism for charge and current neutralization of an HCIB by an electron beam in an axisymmetric accelerating gap was investigated in [3-11]. The physical meaning of the mechanism for charge and current neutralization of an annular HCIB in a magnetically insulated accelerating gap is as follows: the neutralization is provided by a specially injected electron beam, which drifts through the cusp in a self-consistent azimuthal magnetic field and a self-consistent radial electric field that arises from a slight radial separation between the ion and electron beams.

Let the external magnetic field has a cusp axisymmetric configuration,

$$H_r = -H_o I_1(kr)\sin(kz),\ H_z = -H_o I_o(kr)\cos(kz), \quad (1)$$

where r is the transverse coordinate, $z \in [0, L]$ is the longitudinal coordinate, L is the cusp length, $k = \frac{\pi}{L}$, H_0 is the external magnetic field, and $I_o(x)$ and $I_1(x)$ are modified Bessel functions. Let an annular electron beam and annular ion beam of the same cross section and the same current density $|q_e| n_e V_e = q_i n_i V_i$ (where q is the charge of a particle, n and V are the particle density and velocity, and the subscripts "e" and "i" stand for electrons and ions) be injected into a system with a cusp external magnetic field (1) and a longitudinal accelerating electric field E_z. In order for an electron beam to drift through the gap for ion acceleration and, accordingly, to neutralize the charge and current of an HCIB, the electron beam should satisfy the following conditions:

$$|q_e| E_z L < \varepsilon_{oe} << \frac{q_e^2 H_0^2 I_0^2(ka) L^2}{2 m_e c^2}, \quad (2a)$$

$$n_e \le \frac{H_o^2 I_1^2(ka)}{4\pi |q_e| E_z L}\left(\frac{L}{a}\right)^2, \quad (2b)$$

where m_e is the mass of an electron, c is the speed of light, ε_{0e} is the electron kinetic energy. The inequality (2a) means that the electron gyroradius is less than the characteristic cusp length L, and, that the ε_{0e} is higher than the energy lost by the electrons in passing through

the gap. The inequality (2b) means that the magnetic field excited by the azimuthal electron drift is much weaker than the external cusp magnetic field.

The ion beam should be sufficiently high-current to generate a self-consistent azimuthal magnetic and radial electric fields in which electron beam drifts through the cusp with velocity close to ion beam velocity:

$$n_i \geq \frac{H_o^2 I_1^2(ka)}{4\pi\left(\varepsilon_{0e} - |q_e| E_z L\right)}, \quad \Delta \geq \frac{c\Omega_i}{\omega_i^2}, \qquad (3)$$

where $\Omega_i = \frac{q_i H}{m_i c}$ and $\omega_i = \sqrt{4\pi q_i^2 n_i / m_i}$ are the ion gyrofrequency and ion Langmuir frequency, respectively.

In the present paper, we report the results of 2d3v particle-in-cell (PIC) simulations of the transport and acceleration of a high-current tubular ion beam through six magnetoinsulated accelerating gaps. The simulations involve solving a complete set of Maxwell's equations with charge-conserving schemes for calculating the current density on a mesh, and relativistic motion equations for charged particles [9-11].

2. SIMULATION RESULTS

Figure 1 shows the axial cross section of the single cusp accelerating structure under simulation, and the regions where the beams are injected. The multicusp systems to be simulated are formed by connecting additional cusps from the right. The outer boundaries of the system are perfectly conducting metal walls. The length of the cusp is z_L = 5 cm and its radius is r_L = 10 cm. The first one-third of the cusp is the drift space, the second one-third is the accelerating gap, and the third one-third is the drift space. The H_0=7.85 kGs. The accelerating field $|q_e| E_z L_{acc} = 0.9 \cdot \varepsilon_{0e}$ is applied in the first, third, and fifth cusps. In the second half of the accelerating gap an additional high-current electron beam (AHCEB) can be injected in the second, fourth, and sixth cusps. A tubular magnetized electron beam (V_e=0.95c, $n_e = 4.2 \cdot 10^{12}$cm^{-3}) and tubular unmagnetized ion beam (V_i = 0.285c) are injected into the system from the left. The minimum and maximum radii of the beams are r_{min} = 2.75 cm and r_{max} = 3.46 cm, the current densities at the time of injection being equal to one another.

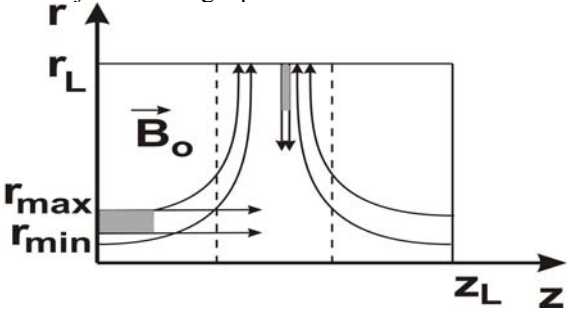

Fig. 1. Configuration of the lines of the external magnetic field and regions of injection of an tubular electron and ion beams, as well as an AHCEB, into the computation domain

Fig. 2 illustrates the results of numerical simulations of the transport (Figs. 2a,b,c) and acceleration (Figs. 2d,e,f) of a HCIB through a six cusps under conditions (2), (3). The AHCEBs was not injected. Shown are the electron (Figs. 2a,d) and ion (Figs. 2b,e) distributions in the $\{r,z\}$ plane, and the ion distribution functions (IDF) $F_i(\varepsilon, r)$ at the right boundary of the last cusp (Figs. 2e,f). From Figs. 2(a,d) we can see that most of the electrons are accompanying the ion beam through all six cusps. But at the center of each cusp, some beam electrons are lost, so the space charge of the ion beam is slightly unneutralized and the ion beam becomes wider (Figs. 2b,e). From Figs. 2(b,c) and 2e,f we can see that, after the passage through the six cusps, the ion beam is slightly divergent and monoenergetic with a kinetic energy of 40.6 MeV (Fig.2c) and 43.6 MeV (Fig. 2f). It should be noted that, as is seen from Figs. 2c and 2f, the IDF over the transverse coordinate is wider in the acceleration case.

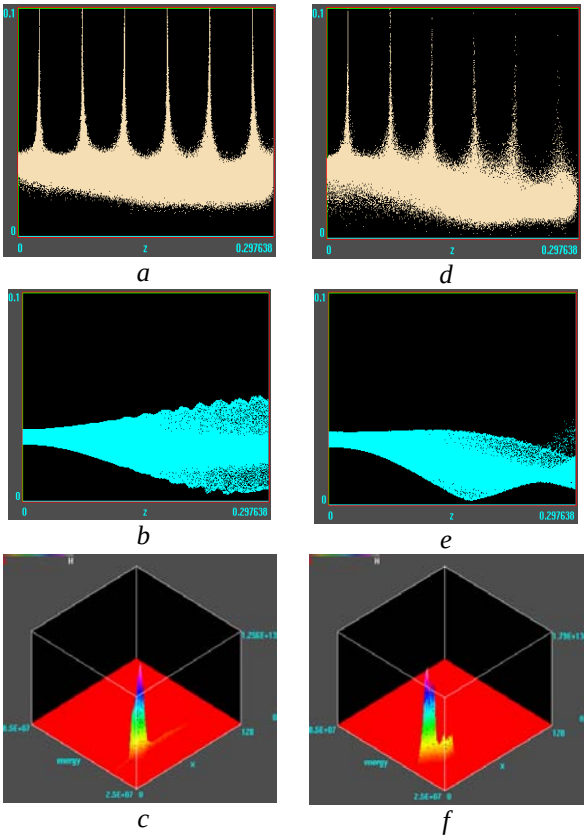

Fig. 2. (a, b, c) transport and (d, e, f) acceleration of a HCIB through six cusps: (a, d) electron and (b, e) ion distributions in the $\{r,z\}$ plane and (c, f) IDF at the right boundary of the sixth cusp

Fig. 3 illustrates the results of simulating the acceleration of a HCIB through six cusps with the additional injection of a cold electron beam into second, fourth, and sixth cusps, where E_z = 0. The parameters of the problem corresponding to Fig. 3 are the same as those in Figs. 2(d,e,f) the only difference being that AHCEBs are injected into cusps. Figs. 3a,c,e correspond to the injection of the AHCEBs which are identical to the main electron beam. Figs. 3(b,d,f) show the simulation results when the optimized over density AHCEBs are injected. The optimization is made to obtain electron densities around accelerated ion beam close to the ion beam densities. Shown are the electron (Figs. 3a,b) and ion (Figs. 3c,d) distributions in the computation region, and

the IDFs at the right boundary of the last cusp (Figs. 3e,f). From Figs. 3(e) and 3(f) we can see that the quality of the IDFs is higher than that in the case without injection of AHCEBs: the accelerated ions are essentially monoenergetic, with an energy of 43.6 MeV, and the divergencies are weaker. From Figs. 3(e) and 3(f) we can also see that the higher the density of the neutralizing electron beams, the better the radial focusing of the accelerated ion beam.

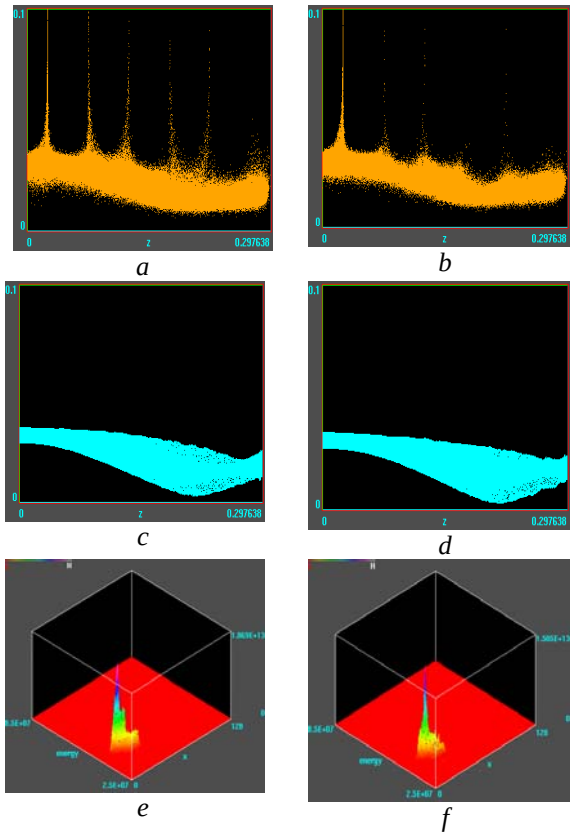

Fig. 3. Acceleration of a HCIB through six cusps with steady injection of an AHCEBs into second, fourth, and sixth cusps, where E_z = 0: (a, b) electron and (c,d) ion distributions in the $\{r,z\}$ plane and (e, f) IDFs at the right boundary of the sixth cusp; (a,c,e) – the AHCEBs densities are $n_e^{add} = 4.2 \cdot 10^{12}$ cm^{-3}, velocities are $V_e^{add} = 0.95c$; (b,d,f) – the AHCEBs densities are $n_e^{add} = 8.4 \cdot 10^{13}$ cm^{-3}, velocities are $V_e^{add} = 0.95c$

Fig. 4 illustrates the results of simulating the acceleration of a HCIB through six cusps with the additional, optimized in time, injection of a cold electron beams into second, fourth, and sixth cusps. The parameters of the problem corresponding to Fig. 4 are the same as those in Fig. 3. The only difference is the injection, optimized in time, of the AHCEBs into cusps. The optimization in the time of injection is made to obtain the simultaneous meeting of the AHCEB heads and ion beam heads in each cusp. Shown are the electron (Figs. 4a,b) and ion (Figs. 4c,d) distributions in the computation domain, and the IDFs at the right boundary of the last cusp (Figs. 4 e,f). From Figs. 4e and 4f we can see that the quality of the IDFs is far higher than that in the case without optimized in the time injection of AHCEBs: the accelerated ions are monoenergetic, with energy of 43.6 MeV, and the divergencies are weaker. From Figs. 4(e) and 4(f) we can see that the optimized in the time injection of the AHCEBs leads to the better radial focusing of the accelerated ion beam.

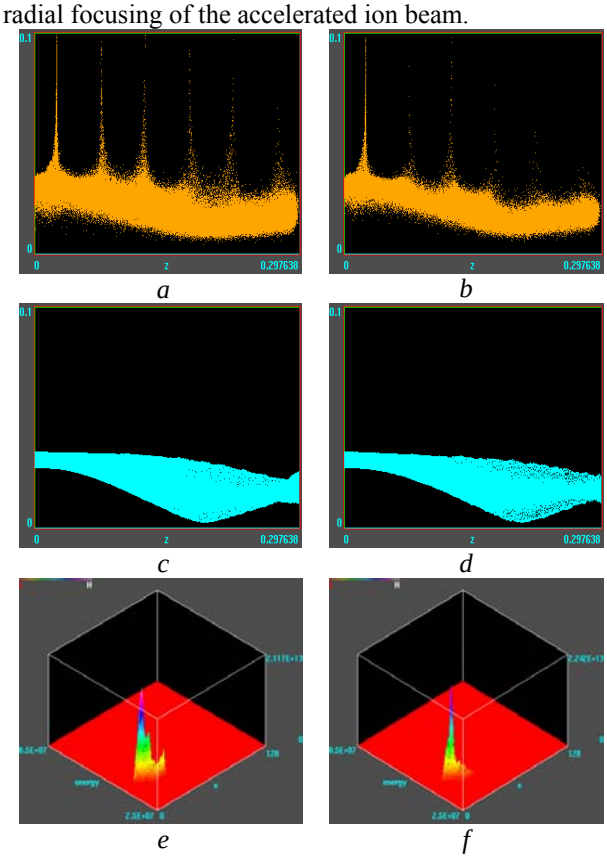

Fig. 4. Acceleration of a HCIB through six cusps with optimized in time injection of an AHCEBs into second, fourth, and sixth cusps: (a, b) electron and (c,d) ion distributions in the $\{r,z\}$ plane and (e, f) IDFs at the right boundary of the sixth cusp; (a,c,e) – the AHCEBs densities are $n_e^{add} = 4.2 \cdot 10^{12}$ cm^{-3}, and velocities are $V_e^{add} = 0.95c$; (b,d,f) – the AHCEBs densities are $n_e^{add} = 8.4 \cdot 10^{13}$ cm^{-3}, $V_e^{add} = 0.95c$

3. CONCLUSIONS

The 2d3v particle-in-cell simulations of the transport and acceleration of a high-current tubular ion beam through six magnetoinsulated accelerating gaps are presented. The ion beam is neutralized by an accompanying electron beam. The accelerating electric fields in the first, third, and fifth cusps are chosen so that electron beam kinetic energy is slightly higher than a potential barrier of the accelerating field in each cusp. The second, fourth, and sixth cusps are used for injection of additional high current electron beams. The accelerating fields in the second, fourth, and sixth cusps are zero. The beam currents, accelerating electric fields, and external magnetic field magnitudes are close to planned experiments. The simulations involve solving a complete set of Maxwell's equations with charge-conserving schemes for calculating the current density on a mesh, and relativistic motion equations for charged particles. It is shown, that at chosen acceleration rates, when the compensating electron beam kinetic energy is slightly

higher than a potential barrier of the accelerating field, the quality of ion distribution function on the accelerator exit is not worsened drastically in comparison with the transportation mode. It is shown, that the optimized in space and time injection of additional high current electron beams in cusps results in increase of accelerated ion beam monochromaticity and to reduction it divergency on an accelerator exit.

REFERENCES

1. *Inertial Confinement Fusion: Current State and Prospects for Power Engineering*/ ed. by B.Yu.Sharkov. Moscow: "Fizmatlit", 2005.
2. O.V. Batishchev, V.I. Golota, V.I. Karas', et al. Linear induction accelerator of charge-compensated ion beams for ICF// *Fiz. Plazmy.* 1993, v. 19, № 5, p. 611-644.
3. V.I. Karas', V.A. Kiyashko, E.A. Kornilov, Ya.B. Fainberg. Theoretical and experimental investigations of neutralized ion induction linac for inertial confinement fusion// *Nuclear Instruments and Methods in Phys. Res. A.* 1989, v. 278, №1, p.245.
4. V.I. Karas', E.A. Kornilov, Ya.B. Fainberg. Linear induction accelerator of charge-compensated ion beams for ICF// *Problems of Atomic Science and Technology. Series "Plasma Electronics and New Methods of Acceleration" (1).* 1998, №1, p.101-107.
5. V.I. Karas', V.V. Mukhin, V.E. Novikov, A.M. Naboka. About compensated ion beam acceleration in magnetoisolated systems// *Fiz. Plazmy.* 1987, v. 13, № 4, p. 494-496.
6. N.G. Belova, V.I. Karas', Yu.S. Sigov. Numerical simulation of charged particle beam dynamics in axial symmetric magnrtic field// *Fiz. Plazmy.* 1990, v. 16, № 2, p. 209-215.
7. N.G. Belova, V.I. Karas'. Optimization of acceleration and charge neutralization of a high-current ion beam in two accelerating gaps of a linear induction accelerator// *Plasma Phys. Rep.* 1995, v. 21, № 12, p. 1005-1013.
8. V.I. Karas', N.G. Belova. Acceleration and stability of high-current ion beams in two accelerating gaps of a linear induction accelerator// *Plasma Phys. Rep.* 1997, v. 23, № 4, p. 328-331.
9. O.V. Bogdan, V.I. Karas', E.A. Kornilov, O.V. Manuilenko. 2.5-d numerical simulation of high-current ion induction linac// *Problems of Atomic Science and Technology. Series "Nuclear Physics Investigations" (49).* 2008, №3. p.34-40.
10. O.V. Bogdan, V.I. Karas', E.A. Kornilov, O.V.Manuilenko. 2.5-dimensional numerical simulation of a high-current ion linear induction accelerator// *Plasma Phys. Rep.* 2008, v. 34, № 8, p. 667-677.
11. O.V. Bogdan, V.I. Karas', E.A.Kornilov, O.V. Manuilenko. Computer simulation of high-current ion induction linac using macroparticles// *Problems of Atomic Science and Technology. Ser. "Plasma Electronics and New Methods of Acceleration" (6).* 2008, №4, p.83-88.

Article received 22.09.08.

СИЛЬНОТОЧНЫЙ ИОННЫЙ ИНДУКЦИОННЫЙ ЛИНАК ДЛЯ ТЯЖЕЛОИОННОГО ИНЕРЦИАЛЬНОГО ТЕРМОЯДЕРНОГО СИНТЕЗА: 2.5-МЕРНОЕ ЧИСЛЕННОЕ МОДЕЛИРОВАНИЕ

О.В. Богдан, В.И. Карась, Е.А. Корнилов, О.В. Мануйленко

Приведены результаты 2.5-мерного численного моделирования методом макрочастиц транспортировки и ускорения сильноточного трубчатого ионного пучка, сопровождаемого компенсирующим электронным пучком, в шести магнитоизолированных ускоряющих промежутках. Ускоряющие электрические поля в первом, третьем и пятом каспах выбраны таким образом, чтобы кинетическая энергия компенсирующего электронного пучка немного превосходила потенциальный барьер ускоряющего поля в каждом каспе. Второй, четвертый и шестой каспы, в которых ускоряющие поля отсутствуют, используются для инжекции дополнительных сильноточных электронных пучков. Моделирования методом макрочастиц выполнены с решением полных уравнений Максвелла с использованием сохраняющей заряд схемы вычисления плотностей тока на сетке, а также с решением релятивистских уравнений движения заряженных частиц. Показано, что при выбранных ускоряющих полях качество функции распределения ионов на выходе ускорителя существенно не ухудшается по сравнению с режимом транспортировки. Показано также, что оптимизированная в пространстве и времени инжекция дополнительных сильноточных электронных пучков в каспы приводит к увеличению монохроматичности и уменьшению расходимости ускоряемого ионного пучка на выходе ускорителя.

СИЛЬНОСТРУМОВИЙ ІОННИЙ ІНДУКЦІЙНИЙ ЛІНАК ДЛЯ ВАЖКОІОННОГО ІНЕРЦІАЛЬНОГО ТЕРМОЯДЕРНОГО СИНТЕЗА: 2.5-ВИМІРНЕ ЧИСЛОВЕ МОДЕЛЮВАННЯ

О.В. Богдан, В.І. Карась, Є.О. Корнілов, О.В. Мануйленко

Наведено результати 2.5-вимірного числового моделювання методом макрочастинок транспортування та прискорення трубчастого сильнострумового іонного пучка, який супроводжується компенсуючим електронним пучком, у шести магнітоізольованих прискорюючих проміжках. Прискорюючі електричні поля у першому, третьому і п'ятому каспах обрано такими, щоб кінетична енергія компенсуючого електронного пучка була трохи більша за потенціальний бар'єр прискорюючого поля у кожному каспі. Другий, четвертий і шостий каспи, в яких прискорюючі поля відсутні, використовуються для інжекції додаткових сильнострумових електронних пучків. Моделювання методом макрочастинок виконано з розв'язанням повних рівнянь Максвелла з використанням зберігаючої заряд схеми обчислення щільності струму на сітці, а також з розв'язанням релятивістських рівнянь руху заряджених частинок. Показано, що при обраних прискорюючих полях якість функції розподілу іонного пучка на виході прискорювача суттєво не погіршується у порівнянні з режимом транспортування. Показано також, що оптимізована у просторі і часі інжекція додаткових сильнострумових

електронних пучків у каспи призводить до збільшення моноенергетичності прискорюємого іонного пучка і до зменшення його розбіжності на виході прискорювача.